RESEARCH ARTICLE

Macromolecular Rapid Communications
www.mrc-journal.de

Synthesis of Bithiazole-Based Poly(arylenevinylene)s via Co-Catalyzed Hydroarylation Polyaddition and Tuning of Their Optical Properties by *N*-Methylation and *N*-Oxidation

*Boya Li, Ryota Iwamori, Junpei Kuwabara, Takeshi Yasuda, and Takaki Kanbara**

Bithiazole-based poly(arylenevinylene) is synthesized via the Co-catalyzed hydroarylation polyaddition of *N*,*N*,*N*′,*N*′-tetrahexyl-(2,2′-bithiazole)-4,4′-dicarboxamide with 2,7-diethynyl-9,9-bis(2-ethylhexyl)fluorene in a regioselective manner. The introduction of the 2,2′-bithiazole unit deepens the highest occupied molecular orbital (HOMO) and lowest unoccupied molecular orbital (LUMO) energy levels of the polymer compared to the analogous bithiophene-based poly(arylenevinylene). *N*-Methylation and *N*-oxidation of the thiazole moiety further deepen the HOMO and LUMO energy levels of the polymer, which is attributed to the enhanced electron-withdrawing effect. The *N*-oxidized polymer exhibits a high photoluminescence quantum yield and serves as an emitting material in an organic light-emitting diode, and its deep HOMO energy level efficiently restrains the trapping of holes in the host poly(vinylcarbazole) matrix.

1. Introduction

Poly(arylenevinylene)s (PAVs) are an attractive family of π-conjugated polymers. Owing to their high planarity, they have been extensively applied as organic optoelectronic materials, particularly organic light-emitting diodes (OLEDs) and organic photovoltaics (OPVs).[1–6] These polymers can be synthesized using several methods.[7,8] A recent promising synthetic approach is polyaddition via hydroarylation of arenes with aromatic diynes, which eliminates the production of byproducts from the monomers.[9–15] We previously demonstrated the Cp*Co(III)-catalyzed hydroarylation polyaddition of *N*,*N*,*N*′,*N*′-tetrahexyl-(2,2′-bithiophene)-4,4′-dicarboxamide with aromatic diynes (**Figure 1a**).[12,15] The amide directing groups facilitated site- and regioselective polyaddition, and the synthesized PAVs served as emitting materials in OLEDs and p-type semiconducting materials in OPVs.

Thiazole is a well-known thiophene analog, which is more electron-deficient than thiophene. Displacement of a bithiophene unit with a bithiazole unit in the π-conjugated polymer structure deepens both the highest occupied molecular orbital (HOMO) and the lowest unoccupied molecular orbital (LUMO) energy levels.[16–20] Owing to intermolecular S···S and S···N interactions, bithiazole-based conjugated polymers tend to exhibit planar structures.[21] In addition, *N*-methylation of the thiazole moiety creates a positive charge on the nitrogen atom, deepening both the HOMO and LUMO energy levels and having a more pronounced effect on the LUMO energy levels. Thus, a narrower bandgap and red-shifted absorption were observed for *N*-methylated bithiazole-based conjugated polymers.[22,23] A similar synthetic strategy was demonstrated by introducing an *N*-oxide group into bithiazole-based conjugated polymers.[24,25] From these observations, we herein designed *N*,*N*,*N*′,*N*′-tetrahexyl-(2,2′-bithiazole)-4,4′-dicarboxamide (**1a**) as a new targeting aromatic monomer for hydroarylation polyaddition (Figure 1b), giving new bithiazole-based PAVs. We anticipated that the introduction of the 2,2′-bithiazole unit would deepen the HOMO and LUMO energy levels of PAVs compared to the bithiophene-based analogs. In addition, *N*-methylation and *N*-oxidation of the thiazole moiety led to the generation of electron-deficient polymer backbones (Figure 1c). The *N*-oxidized PAV has a high photo-

B. Li, R. Iwamori, J. Kuwabara, T. Kanbara
Institute of Pure and Applied Sciences
University of Tsukuba
1-1-1 Tennodai, Tsukuba, Ibaraki 305–8573, Japan
E-mail: kanbara@ims.tsukuba.ac.jp
J. Kuwabara
Tsukuba Research Center for Energy Materials Science (TREMS)
Institute of Pure and Applied Sciences
University of Tsukuba
1-1-1 Tennodai, Tsukuba, Ibaraki 305–8573, Japan
T. Yasuda
Research Center for Macromolecules and Biomaterials
National Institute for Materials Science (NIMS)
1-2-1 Sengen, Tsukuba, Ibaraki 305-0047, Japan

The ORCID identification number(s) for the author(s) of this article can be found under https://doi.org/10.1002/marc.202401082

[The copyright line for this article was changed on 12 February 2025 after original online publication.]

DOI: 10.1002/marc.202401082

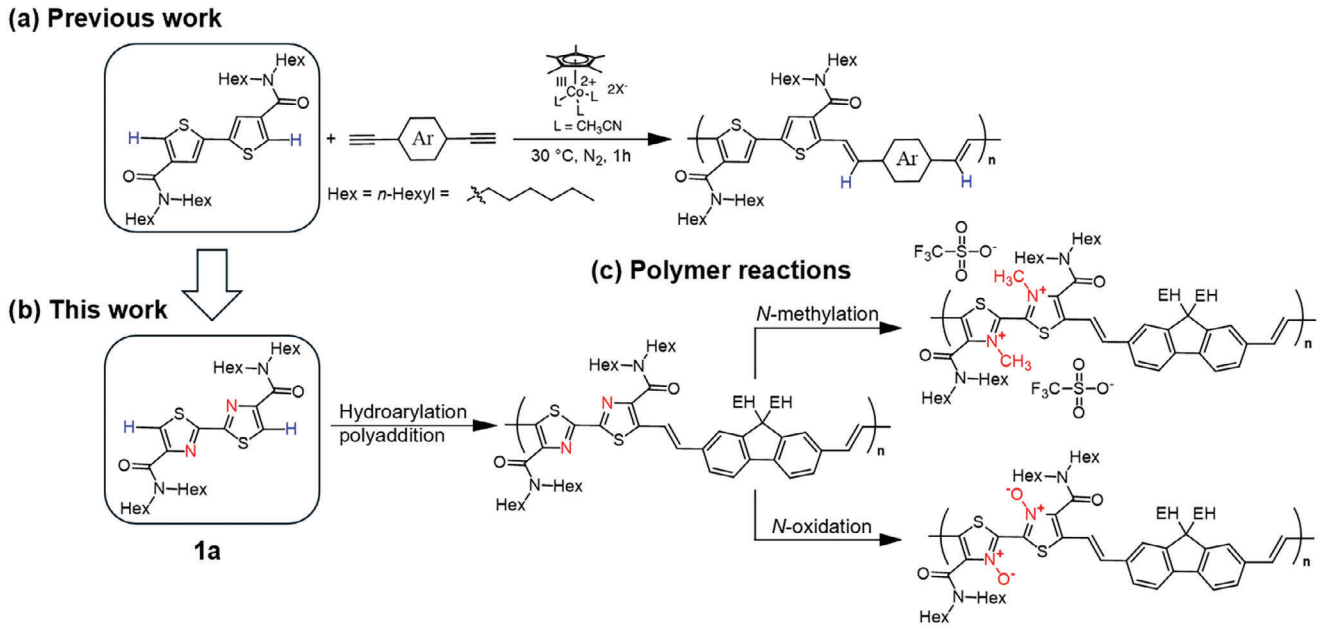

Figure 1. Co-catalyzed hydroarylation polyaddition and polymer reactions.

luminescence property as well as a deep HOMO energy level, which contributes to its electroluminescence property as a guest-emitting material for OLEDs.

2. Results and Discussion

2.1. Model Reaction

To assess the reactivity of **1a**, we conducted a small molecular model reaction, as described in our previous study.[12] The hydroarylation of **1a** with 4-ethynyltoluene (**2a**) was performed in dry 1,2-dichloroethane (DCE, 0.05 M) at 30 °C in the presence of $[Cp^*Co(CH_3CN)_3](SbF_6)_2$ (2 mol%) and neodecanoic acid (NDA, 30 mol%) (**Scheme 1**). The conversion of **1a** to dialkenylated product (**3aa**) was confirmed by time-course analyses using nuclear magnetic resonance (NMR) spectroscopy. The NMR yield of **3aa** reached 60% after 1 h, and quantitative consumption of **1a** was achieved after 24 h (Figure S1, Supporting Information). The reactivity of **1a** was slightly lower than that of its analogous bithiophene monomer. The presence of electron-withdrawing nitrogen atoms weakened the ability of the carbonyl oxygen in the amide groups to coordinate with the Co catalyst. This feature lowers the reactivity of the concerted metalation-deprotonation (CMD) step, which is the rate-determining step in the catalytic cycle of hydroarylation (Scheme S1, Supporting Information). Nevertheless, the hydroarylation reaction proceeded selectively at the 5,5′-positions of **1a**; **3aa** was isolated as the *E,E*-isomer in 81% yield (Figure S2, Supporting Information). These results indicate that **1a** applies to hydroarylation polyadditions with a longer reaction time than the analogous bithiophene monomer.

2.2. Polyaddition Reaction

Subsequently, the hydroarylation polyaddition of **1a** with 2,7-diethynyl-9,9-bis(2-ethylhexyl)fluorene (**4a**) was performed under the same reaction conditions as the small molecular model reaction (**Scheme 2**). The reaction was quenched after 4 h, as the reaction mixture became viscous. The corresponding PAV (**Paa**) was obtained in 91% yield with a number-average molecular weight (M_n) of 40000 and a polydispersity index (M_w/M_n) of 2.8, which

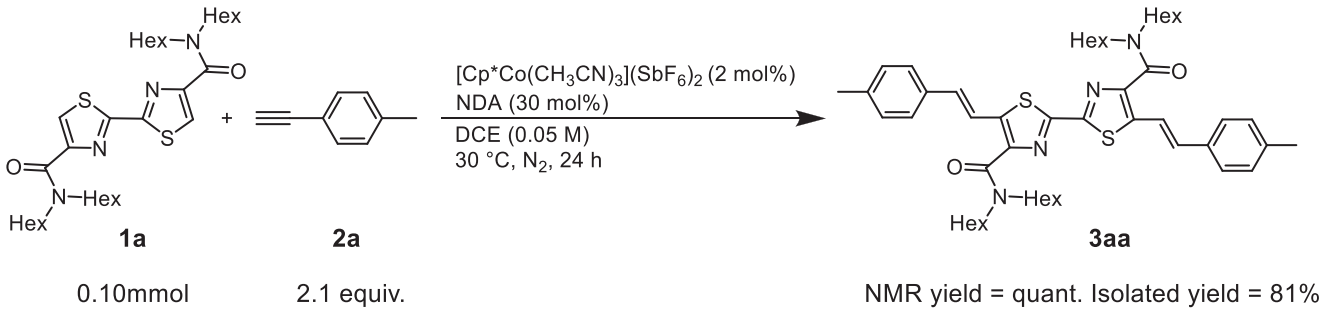

Scheme 1. Small molecular model reaction of 1a with 2a.

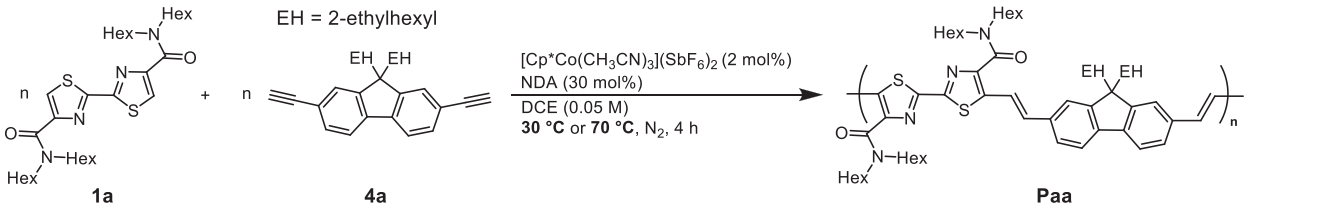

Scheme 2. Hydroarylation polyaddition of 1a with 4a.

were estimated by gel permeation chromatography (GPC). When the reaction temperature was raised to 70 °C, the polyaddition reaction gave **Paa** in 92% yield, with an M_n of 77000 and M_w/M_n of 3.0 (Figure S13a, Supporting Information). All signals in the ^{1}H NMR spectrum of **Paa** were assigned to the repeating structure with a 1,2-vinylene unit and to each terminal structure (**Figure 2**); there was no minor signal derived from the 1,1-vinylidene unit (5.5–5.0 ppm). To check the monomer scope of the reactions with **1a**, we also conducted the hydroarylation polyaddition of **1a** with 2,7-bis(4-ethynylphenyl)-9,9-di(*n*-octyl)fluorene (**4b**) (Scheme S2, Figure S3, Supporting Information). The reactivity of the diyne monomer was increased by introducing a phenylene spacer between the alkyne and fluorene moieties, resulting in a high yield and molecular weight within a reaction time of only 10 min (Figure S13b, Supporting Information). **Paa** and **Pab** were also synthesized at different temperatures and reaction times, yielding the corresponding PAVs with reasonable molecular weights in good yields (Table S1, Supporting Information).

2.3. Polymer Reactions

Methyl trifluoromethanesulfonate (MeOTf), a strong methylating reagent, is commonly used for *N*-methylation of thiazole derivatives.[22,23] Therefore, we selected MeOTf to perform the *N*-methylation of **Paa** (M_n = 77 000). According to a previous report,[22] the reaction was carried out for 7 d in dry chloroform at 50 °C using 7 equiv. of MeOTf (**Table 1**, Entry 2, and Scheme S3, Supporting Information). The *N*-methylated product **Paa-M** was purified and obtained in 65% yield, calculated based on the *N*-methylation ratio. From the ^{1}H NMR analysis of **Paa-M**, the signal derived from *N*—CH_3 of methylated thiazole unit was confirmed at δ 4.54 ppm. The *N*-methylation ratio was calculated from the integral ratio of the signals of aromatic C—H bonds (10H at δ 8.2–7.2 ppm) to those of *N*—CH_3 (maximum value = 6H), resulting in 37% modification (Figure S4, Supporting Information for the detail of calculation method). The *N*-methylation ratio was also calculated from the α-methylene protons of the alkyl amides (8H at δ 4.0–3.2 ppm) to *N*—CH_3; the value was the same as that from aromatic C—H bonds. Further structural analysis was conducted using Fourier transform infrared (FT–IR) spectroscopy. The FT–IR spectrum showed strong infrared vibration bands of triflate ions at 1262, 1160, 1033, and 638 cm^{-1} (Figure S11, Supporting Information).[22,23] **Paa-M** with different methylation ratios were obtained by changing the reaction temperature and feeding amount of MeOTf (Table 1 and Figures S5–S7, Supporting Information). Increasing the amount of MeOTf initially increased the methylation ratio (Entries 1 and 2); however, excess MeOTf decreased the methylation ratio (Entry 3). Higher reaction temperatures also increased the methylation ratio (Entry 4). Due to the steric hindrance caused by the amide side chains of the bithiazole backbone, introducing *N*—CH_3 at both sites is considered challenging, exceeding 50% of the *N*-methylation ratio is difficult.

Subsequently, the *N*-oxidation reaction of **Paa** (M_n = 77 000) was performed. Based on the literature,[24] the reaction was conducted using 6 equiv. of *meta*-chloroperoxybenzoic acid (*m*-CPBA) in dry DCE at 30 °C for 96 h (Scheme S4, Supporting Information). Insoluble solids precipitated from the reaction mixture. The *N*-oxidation product **Paa-O** was purified and obtained in 56% yield, which was calculated based on the *N*-

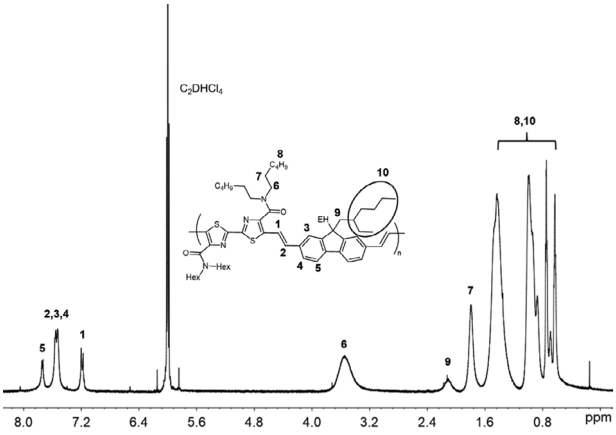

Figure 2. ^{1}H NMR spectrum of Paa (M_n = 77000, 600 MHz, $C_2D_2Cl_4$, 373 K).

Table 1. Results of *N*-methylation reaction of Paa.

Entry[a)]	PAVs	MeOTf equiv.	Temp./°C	Yield[b)] /%	*N*-methylation ratio[c)] /%
1	Paa-M-11	3.5	50	69	11
2	Paa-M-37	7	50	65	37
3	Paa-M-27	14	50	62	27
4	Paa-M-50	7	70	66	50

[a)] Paa (M_n = 77 000, 0.02 mmol) was reacted with MeOTf (prescribed equivalent) in $CHCl_3$ (0.01 M) at the prescribed temperature for 7 d; [b)] The yields were calculated based on the *N*-methylation ratio; [c)] Calculated from the ^{1}H NMR spectra using acetone-d_6 at room temperature.

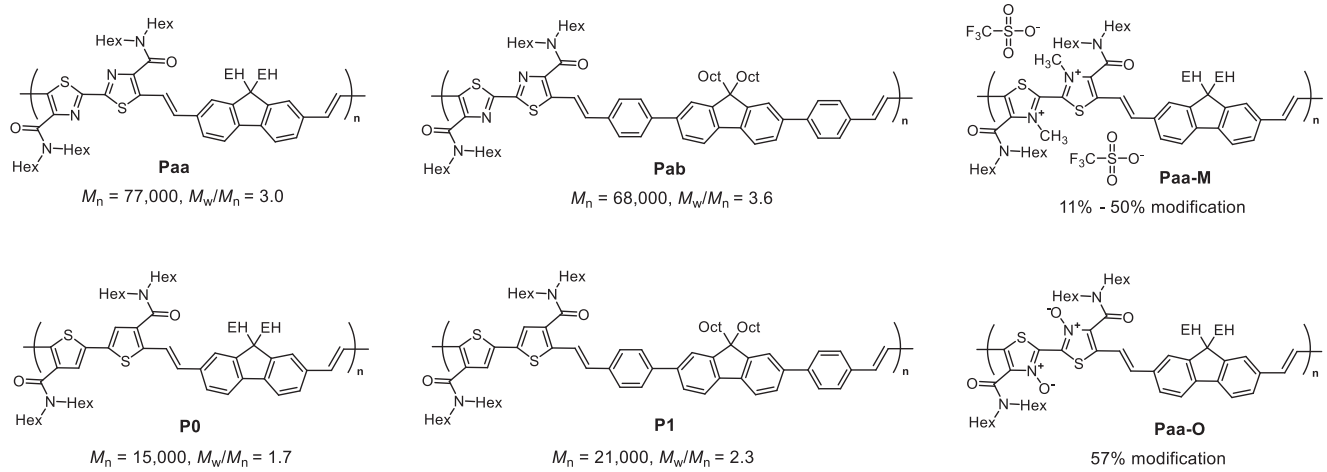

Figure 3. Chemical structures of PAVs.

oxidation ratio. Because **Paa-O** showed high solubility only in THF, the ^{1}H NMR spectrum of **Paa-O** was measured using a solvent mixture of THF:$CDCl_3$ = 1:1. From the ^{1}H NMR analysis of **Paa-O**, the signal derived from the α-methylene protons of dialkyl amides was confirmed at δ 5.8–4.8 ppm. These signals exhibit significant downfield shifts, which are attributed to the electron-withdrawing effect of *N*-oxidation. The *N*-oxidation ratio was calculated from the integral ratio of the vinylene structure (2H at δ 7.0–6.7 ppm) to that of the α-methylene protons of dialkyl amides (maximum value = 8H), resulting in 57% modification (Figure S8, Supporting Information for details of the calculation method). Further structural analysis was conducted using FT–IR spectroscopy, which showed strong infrared vibration bands of the N—O bond at 1163 cm^{-1} (Figure S12, Supporting Information).[26,27]

2.4. Optical Properties

The optical properties of the synthesized PAVs were investigated. The structures of the PAVs subjected to optical properties are shown in **Figure 3**. First, we discuss the optical spectra of the PAVs in dilute solutions (**Figure 4** and Table S2, Supporting Information). In $CHCl_3$ solution, the ultraviolet-visible (UV–vis) absorption and photoluminescence (PL) spectra of **Paa** exhibited redshifts compared to the analogous bithiophene polymer **P0**, attributed to the rigid and planar structure of the bithiazole backbone (Figure S14, Supporting Information). A similar trend was observed for **Pab** compared to **P1** (Figure S15, Supporting Information). As the *N*-methylation ratio of **Paa-M** increased, the absorption intensity of the original **Paa** decreased, and a long-wavelength absorption band (550–600 nm) emerged (Figure 4a). This result is similar to those reported in the literature.[22,23] In our experiment, even a small amount of *N*-methylation can significantly affect the overall π-conjugated system of the polymer, leading to disproportionate changes in the absorption bands. The PL spectra of **Paa-M** also red-shifted compared with those of **Paa** (Figure S16, Supporting Information). The photoluminescence quantum yield (PLQY) of **Paa-M** was lower than that of **Paa** but gradually increased with the degree of *N*-methylation (Table S2, Supporting Information). The UV–vis absorption spectrum of **Paa-O** in THF showed a blue shift compared to that of **Paa** (Figure 4b). The *N*-oxidized bithiazole-based conjugated polymers typically exhibit redshifts in absorption compared with the original polymers.[24,25] However, alternation of the side chains of the *N*-oxidized polymers from alkyl to amide groups resulted in blue-shifted absorption, which was considered to limit the effective conjugation length.[27] **Paa-O** exhibited a similar λ_{em} to **Paa** and maintained a high PLQY (Figure S17, Supporting Information).

The optical properties of the PAVs in the film state were compared with those in a dilute solution (**Table 2**, **Figure 5**a). For

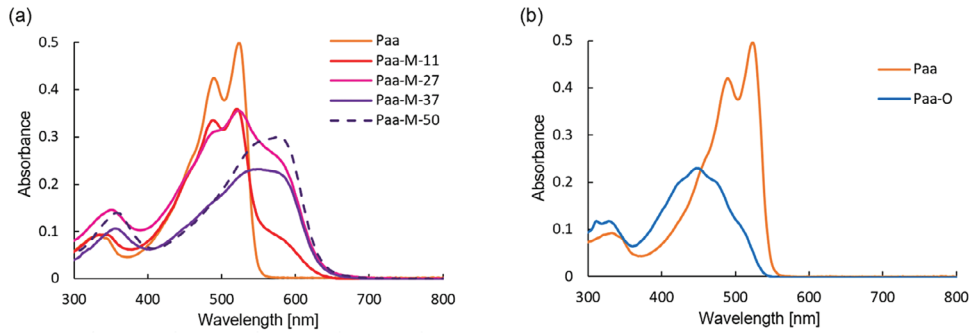

Figure 4. UV–vis absorption spectra of a) Paa and Paa-M in the $CHCl_3$ solution (5.0×10^{-6} M) and b) Paa and Paa-O in the THF solution (5.0×10^{-6} M).

Table 2. The optical properties of PAVs in the film states.

PAVs	λ_{max} /nm	λ_{edge} /nm	E_g^{opt} [a] /eV	E_{HOMO} [b] /eV	E_{LUMO} [c] /eV	PLQY [d] /%
P0	490	549	2.26	−5.31	−2.71	10.7
Paa	530	553	2.24	−5.52	−2.99	13.6
Paa-O	452	540	2.30	−5.77	−3.15	23.7
Paa-M-27	529	624	1.99	−5.80	−3.63	7.4
Paa-M-50	556	626	1.98	−5.80	−3.64	7.6

[a] Optical bandgap from the absorption edge; [b] E_{HOMO} was determined by UPS; [c] E_{LUMO} was determined by LEIPS; [d] Photoluminescence quantum yield.

Paa-M, no notable shifts were observed in either the absorption or the PL spectra between the film and solution states (Figure S18, Supporting Information). In contrast, **Paa** and **Paa-O** exhibited significant redshifts in their PL spectra, by 56 and 60 nm, respectively, while no significant shifts in λ_{max} were observed in their absorption spectra between the film and solution states (Figure S18, Supporting Information). The PLQY of all the PAVs decreased in the film state compared to that in the solution state because of aggregation-caused quenching (ACQ),[13,28,29] whereas **Paa-O** film retained a relatively high PLQY of 23.7%. The optical bandgap (E_g^{opt}) of each PAV in the film state was calculated using the absorption edge. *N*-methylation narrowed the E_g^{opt} by 0.3 eV compared to the original **Paa**, while **Paa-O** exhibited a wider E_g^{opt} than **Paa**.

The HOMO and LUMO energy levels (E_{HOMO} and E_{LUMO}) of the PAVs in the thin films were measured using ultraviolet photoelectron spectroscopy (UPS) and low-energy inverse photoelectron spectroscopy (LEIPS),[30] respectively (Table 2, Figures 5b and S19–S25, Supporting Information). Compared with bithiophene-based PAV (**P0**),[12] the frontier orbital energy levels of bithiazole-based **Paa** became deeper by 0.2 eV owing to the electron-withdrawing effect of bithiazole moiety. The relationship between the energy levels of **P1** and **Pab** was consistent with that between **P0** and **Paa** (Figure S26, Supporting Information). The *N*-methylation of **Paa** effectively deepened both E_{HOMO} and E_{LUMO}, especially the E_{LUMO} by 0.6 eV. As the LUMO of **Paa** mainly resided at the nitrogen atoms on the bithiazole moiety,[22] the E_{LUMO} of **Paa-M** was further deepened compared to that of the E_{HOMO} owing to the electron-withdrawing effect, even with a low *N*-methylation ratio. The frontier orbital energy levels of **Paa-M-27** were approximately the same as those of **Paa-M-50**. Although the λ_{max} of **Paa-M** red-shifted with increasing *N*-methylation ratio, the E_g^{opt}, E_{HOMO}, and E_{LUMO} of **Paa-M** remained constant owing to the unchanged absorption edge. The *N*-oxidation of **Paa** also deepened both E_{HOMO} and E_{LUMO}. However, the E_{LUMO} of **Paa-O** was shallower than that of **Paa-M** by 0.5 eV.

2.5. OLED Properties

Because the **Paa-O** film exhibited a high PLQY in both the dilute solution and film states, the electroluminescent (EL) properties of the OLED were evaluated. Poly(vinylcarbazole) (PVK) with 2.9 wt% **Paa-O** in THF was spin-coated to form a hole-transport PVK film doped with **Paa-O** (see Supporting Information for details of OLED fabrication). Because of the large overlap between the PL spectrum of the PVK thin film and the absorption spectrum of the **Paa-O** solution (Figure S27, Supporting Information), the exciton energy of PVK is expected to be transferred to **Paa-O** via Förster resonance energy transfer.[31–35] Efficient emissions can be obtained from excited **Paa-O** by doping a small amount of **Paa-O** into a PVK thin film. The EL spectrum in **Figure 6** was representative of ≈10 cd m^{-2}, and the coordinates of the CIE chromaticity diagram were $x = 0.437$ and $y = 0.528$ (Figure S28, Supporting Information). The current efficiency reached 6.42 cd A^{-1} at a current density of 0.412 mA cm^{-2}, and the maximum external quantum efficiency (EQE) of the OLED was 2.10% (Figure S29, Supporting Information). The EQE of

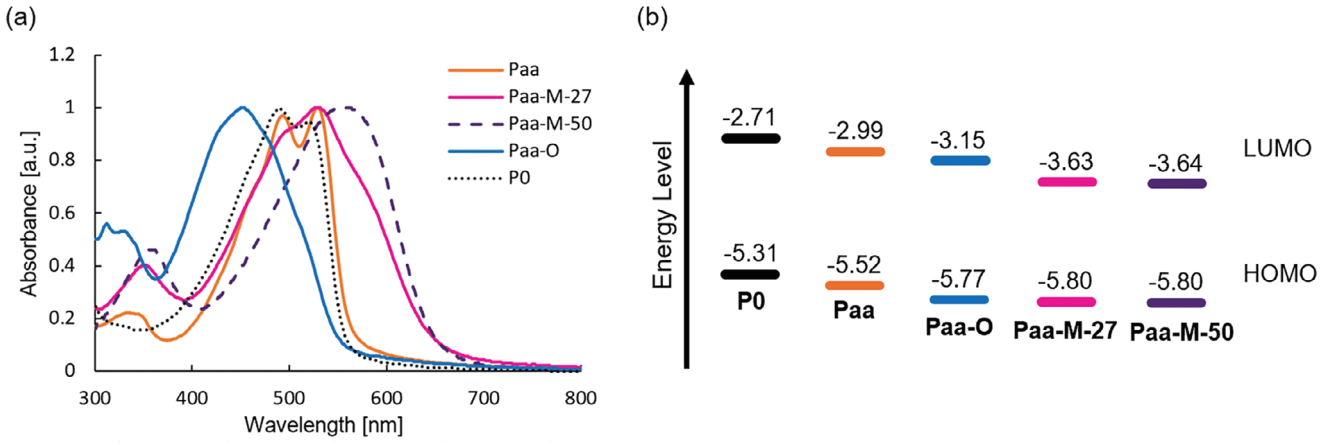

Figure 5. a) UV–vis absorption spectra of Paa, Paa-M, and Paa-O in film states. b) Energy level diagram of PAVs.

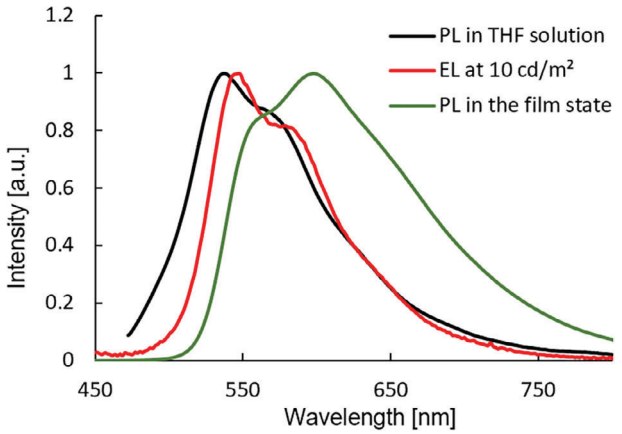

Figure 6. PL and EL spectra of Paa-O.

the OLED with the same structure, where **Paa-O** was replaced with **Paa**, was 1.39%. The EL spectrum was similar to the PL spectrum of **Paa-O** in dilute solution, whereas no emission peaks corresponding to PVK and **Paa-O** in the film states were observed (Figure 6). As expected, this behavior shows that **Paa-O** dispersed in the PVK layer was efficiently excited by the Förster resonance energy transfer of the exciton energy of PVK. The relationship between the HOMO energy levels of the dopant and host matrix is generally important for the hole mobilities of the host matrix.[36,37] In our experiments, the HOMO energy level of **Paa-O** was nearly the same as that of PVK (−5.76 eV); therefore, it appears that **Paa-O** does not act as a hole trap in the PVK layer, i.e., doping a small amount of **Paa-O** into PVK does not reduce the hole mobility of PVK (Figure S30, Supporting Information).

3. Conclusion

In summary, bithiazole-based poly(arylenevinylene)s were synthesized via Co-catalyzed hydroarylation polyaddition, followed by *N*-methylation and *N*-oxidation via polymer reactions. The optical spectra of the synthesized bithiazole-based PAVs were red-shifted compared with those of their bithiophene-based analogs. *N*-Methylation of bithiazole-based **Paa** resulted in further red-shifted absorption and narrow bandgaps, whereas *N*-oxidation of **Paa** induced blue-shifted absorption. The HOMO and LUMO energy levels of the bithiazole-based PAVs were deeper than those of the corresponding bithiophene-based analogs, owing to the electron-withdrawing properties of the bithiazole units. *N*-Methylation further deepened the LUMO energy level, whereas *N*-oxidation deepened the LUMO and HOMO energy levels. Therefore, the *N*-modification serves as a promising tool for tuning a wide range of PAV optical properties and energy levels. Notably, **Paa-O** exhibited a high PLQY and a deep HOMO energy level, highlighting its potential as a guest-emitting material for OLEDs.

4. Experimental Section

*Synthesis of **Paa***: To a stirred solution of **1a** (177.28 mg, 0.30 mmol) and **4a** (131.61 mg, 0.30 mmol) in anhydrous DCE (6.0 mL) were added $[Cp^*Co(CH_3CN)_3](SbF_6)_2$ (4.73 mg, 0.0060 mmol) and NDA (17.0 µL, 0.090 mmol). The reaction mixture was stirred for 4 h at 70 °C under a nitrogen atmosphere. Then, the reaction mixture was diluted with $CHCl_3$ (50 mL) and poured into an NH_3 solution (28% in water, 50 mL). The organic layer was washed with NH_3 solution and distilled water (100 mL × 2). The organic layer was dried over sodium sulfate and filtered through a Celite plug. The solution of $CHCl_3$ was concentrated and reprecipitated into methanol. The precipitate was collected by filtration and dried under a vacuum. A polymeric product (**Paa**) was obtained as an orange solid in 92% yield (283.4 mg, M_n = 77000, M_w/M_n = 3.0). ^{1}H NMR (600 MHz, $C_2D_2Cl_4$, 373 K): δ = 7.74 (d, J = 9.8, 2H), 7.54 (m, 6H), 7.19 (d, J = 15.1, 2H), 3.55 (br s, 8H), 2.12 (br s, 4H), 1.80 (br s, 8H), 1.39 (br s, 24H), 0.27–1.15 (m, 42H). Anal. calcd. for $C_{65}H_{96}N_4O_2S_2$: C 75.82, H 9.40, N 5.44; found: C 74.70, H 9.73, N 5.42.

Pab was obtained by the same procedure. (Supporting Information)

*Synthesis of **Paa-M-37***: A solution of **Paa** (20.59 mg, 0.020 mmol based on the repeating unit) and MeOTf (15.8 µL, 0.14 mmol) in anhydrous $CHCl_3$ (2.0 mL) was stirred for 7 days at 50 °C under a nitrogen atmosphere. During the reaction, the color of the solution gradually changed from orange to red and ultimately to purple. The reaction product was concentrated and reprecipitated into hexane. The precipitate was washed with water and dried under a vacuum. An *N*-methylated product (**Paa-M-37**) was obtained as a purple solid in 65% yield. (calculated based on the *N*-methylation ratio, 15 mg) ^{1}H NMR (600 MHz, Acetone-d_6, r.t.): δ = 7.22–8.18 (m, 10H, aromatic C—H bonds), 4.36–4.69 (s, 2.22H, *N*—CH_3), 3.17–3.86 (m, 8H, α-methylene protons of alkyl amides). 2.15 (br s, 8H), 1.61–1.98 (m, 8H), 1.10–1.58 (m, 24H), 0.37–1.08 (m, 42H). The *N*-methylation ratio = 37%

Paa-M-11, **Paa-M-27**, and **Paa-M-50** were obtained by the same procedure. (Supporting Information)

*Synthesis of **Paa-O***: A solution of **Paa** (61.78 mg, 0.060 mmol based on the repeating unit) and *m*-CPBA (62.13 mg, 0.36 mmol) in anhydrous DCE (3.0 mL) was stirred for 96 h at 30 °C under a nitrogen atmosphere. During the reaction, insoluble solids in DCE were observed precipitating from the reaction mixture. After removing DCE, the precipitate was washed three times with hexane and dried under vacuum. An *N*-oxidized product (**Paa-O**) was obtained as an orange solid in 56% yield. (calculated based on the *N*-oxidation ratio, 35.4 mg) ^{1}H NMR (600 MHz, THF: $CDCl_3$ = 1:1, r.t.): δ = 7.04–7.63 (m, 8H), 6.75–7.00 (m, 2H, the vinylene structure), 4.86–5.79 (m, 4.56H, the α-methylene protons of alkyl amides after *N*-oxidation). The *N*-oxidation ratio = 57%

Supporting Information

Supporting Information is available from the Wiley Online Library or from the author.

Acknowledgements

The authors thank the Chemical Analysis Division and the OPEN FACILITY, Research Facility Center for Science and Technology, University of Tsukuba, for the measurements of NMR, APCI-MS, LEIPS, and UPS. The LEIPS and UPS measurements were supported by "Advanced Research Infrastructure for Materials and Nanotechnology in Japan (ARIM)" of the Ministry of Education, Culture, Sports, Science, and Technology (MEXT); proposal number JPMXP1224BA0038. The authors are grateful to Dr. Ayako Okano for fruitful discussions about the LEIPS and UPS measurements. This work was partly supported by JSPS KAKENHI Grant Numbers 23K04835 and 23KJ0240.

Conflict of Interest

The authors declare no conflict of interest.

Data Availability Statement

The data that support the findings of this study are available from the corresponding author upon reasonable request.

Keywords

bithiazole, conjugated polymer, energy level, hydroarylation, polyaddition, polymer reaction

Received: December 16, 2024
Revised: January 23, 2025
Published online: February 7, 2025

[1] L. Ding, Z. Di Yu, X. Y. Wang, Z. F. Yao, Y. Lu, C. Y. Yang, J. Y. Wang, J. Pei, *Chem. Rev.* **2023**, *123*, 7421.
[2] Y. Wang, T. Hasegawa, H. Matsumoto, T. Michinobu, *J. Am. Chem. Soc.* **2019**, *141*, 3566.
[3] A. C. Grimsdale, K. L. Chan, R. E. Martin, P. G. Jokisz, A. B. Holmes, *Chem. Rev.* **2009**, *109*, 897.
[4] J. H. Burroughes, D. D. C. Bradley, A. R. Brown, R. N. Marks, K. Mackay, R. H. Friend, P. L. Burns, A. B. Holmes, *Nature* **1990**, *347*, 539.
[5] A. Kraft, A. C. Grimsdale, A. B. Holmes, *Angew. Chem., Int. Ed.* **1998**, *37*, 402.
[6] C. Yang, S. Zhang, J. Hou, *Aggregate* **2022**, *3*, e111.
[7] A. J. Blayney, I. F. Perepichka, F. Wudl, D. F. Perepichka, *Isr. J. Chem.* **2014**, *54*, 674.
[8] T. Junkers, J. Vandenbergh, P. Adriaensens, L. Lutsen, D. Vanderzande, *Polym. Chem.* **2012**, *3*, 275.
[9] S. Selmani, L. Vanderzwet, A. J. Kukor, D. J. Schipper, *Synlett* **2018**, *29*, 2552.
[10] E. R. King, J. Tropp, N. Eedugurala, L. E. Gonce, S. Stanciu, J. D. Azoulay, *Angew. Chem., Int. Ed.* **2020**, *59*, 21971.
[11] R. Iwamori, R. Sato, J. Kuwabara, T. Yasuda, T. Kanbara, *Macromol. Rapid Commun.* **2021**, *42*, 2100283.
[12] R. Iwamori, J. Kuwabara, T. Yasuda, T. Kanbara, *Macromolecules* **2023**, *56*, 5407.
[13] R. Iwamori, J. Kuwabara, T. Yasuda, T. Kanbara, *Macromol. Rapid Commun.* **2024**, *45*, 2400168.
[14] K. Tsukahara, R. Iwamori, J. Kuwabara, T. Kanbara, *Macromol. Rapid Commun.* **2024**, *45*, 2400456.
[15] R. Iwamori, K. Miyata, J. Kuwabara, T. Yasuda, T. Kanbara, *Synth. Met.* **2025**, *311*, 117817.
[16] M. Ji, C. Dong, Q. Guo, M. Du, Q. Guo, X. Sun, E. Wang, E. Zhou, *Macromol. Rapid Commun.* **2023**, *44*, 2300102.
[17] Y. Wang, T. Hasegawa, H. Matsumoto, T. Mori, T. Michinobu, *Adv. Funct. Mater.* **2017**, *27*, 1604608.
[18] Y. Shi, H. Guo, M. Qin, Y. Wang, J. Zhao, H. Sun, H. Wang, Y. Wang, X. Zhou, A. Facchetti, X. Lu, M. Zhou, X. Guo, *Chem. Mater.* **2018**, *30*, 7988.
[19] Y. Shi, W. Li, X. Wang, L. Tu, M. Li, Y. Zhao, Y. Wang, Y. Liu, *Chem. Mater.* **2022**, *34*, 1403.
[20] Y. Teshima, M. Saito, T. Mikie, K. Komeyama, I. Osaka, *Macromolecules* **2021**, *54*, 3489.
[21] M. Kuramochi, J. Kuwabara, W. Lu, T. Kanbara, *Macromolecules* **2014**, *47*, 7378.
[22] J. K. Politis, M. D. Curtis, Y. He, J. Kanicki, *Macromolecules* **1999**, *32*, 2484.
[23] M. D. Curtis, H. Cheng, J. A. Johnson, J. I. Nanos, R. Kasim, R. L. Elsenbaumer, L. G. Ronda, D. C. Martin, *Chem. Mater.* **1998**, *10*, 13.
[24] X. He, F. Ye, J. C. Guo, W. Chang, B. Ma, R. Ding, S. Wang, Y. Liang, D. Hu, Z. H. Guo, Y. Ma, *Polym. Chem.* **2023**, *14*, 1945.
[25] G. S. Sinclair, R. C. M. Claridge, A. J. Kukor, W. S. Hopkins, D. J. Schipper, *Chem. Sci.* **2021**, *12*, 2304.
[26] L. C. Campeau, M. Bertrand-Laperle, J. P. Leclerc, E. Villemure, S. Gorelsky, K. Fagnou, *J. Am. Chem. Soc.* **2008**, *130*, 3276.
[27] T. Yamamoto, B.-L. Lee, H. Hayashi, N. Saito, T. Maruyama, *Polymer* **1997**, *38*, 4233.
[28] X. Ma, R. Sun, J. Cheng, J. Liu, F. Gou, H. Xiang, X. Zhou, *J. Chem. Educ.* **2016**, *93*, 345.
[29] J. H. Hsu, *J. Phys. Chem. A* **1999**, *103*, 2375.
[30] A. Sugie, K. Nakano, K. Tajima, I. Osaka, H. Yoshida, *J. Phys. Chem. Lett.* **2023**, *14*, 11412.
[31] F. Laquai, Y.-S. Park, J.-J. Kim, T. Basché, *Macromol. Rapid Commun.* **2009**, *30*, 1203.
[32] J. Kido, K. Hongawa, K. Okuyama, K. Nagai, *Appl. Phys. Lett.* **1994**, *64*, 815.
[33] E. G. Thianche, C. Sentein, A. Lorin, C. Denis, P. Raimond, J. M. Nunzi, *J. Appl. Phys.* **1998**, *83*, 4236.
[34] R. Zhang, H. Zheng, J. Shen, *Synth. Met.* **1999**, *105*, 49.
[35] U. Deori, G. P. Nanda, C. Murawski, P. Rajamalli, *Chem. Sci.* **2024**, *15*, 17739.
[36] D. M. Pai, J. F. Yanus, M. Stolka, *Phys. Chem.* **1984**, *88*, 4714.
[37] N. Altinolcek, A. Battal, M. Tavasli, J. Cameron, W. J. Peveler, H. A. Yu, P. J. Skabara, *Synth. Met.* **2020**, *268*, 116504.

